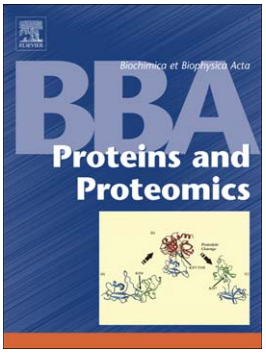

Insights into the functional properties of the marneral oxidase CYP71A16 from *Arabidopsis thaliana*

Sarah Kranz-Finger, Osama Mahmoud, Esther Ricklefs, Nikolas Ditz, Patrick J. Bakkes, Vlada B. Urlacher

PII: S1570-9639(17)30163-2
DOI: doi:10.1016/j.bbapap.2017.07.008
Reference: BBAPAP 39973

To appear in: *BBA - Proteins and Proteomics*

Received date: 7 April 2017
Revised date: 12 July 2017
Accepted date: 18 July 2017

Please cite this article as: Sarah Kranz-Finger, Osama Mahmoud, Esther Ricklefs, Nikolas Ditz, Patrick J. Bakkes, Vlada B. Urlacher, Insights into the functional properties of the marneral oxidase CYP71A16 from *Arabidopsis thaliana*, *BBA - Proteins and Proteomics* (2017), doi:10.1016/j.bbapap.2017.07.008

Insights into the functional properties of the marneral oxidase CYP71A16 from *Arabidopsis thaliana*

Sarah Kranz-Finger[a,b], Osama Mahmoud[a], Esther Ricklefs[a], Nikolas Ditz[a,b], Patrick J. Bakkes[a], Vlada B. Urlacher*[a,b]

Dedicated to the 75th anniversary of Professor Rolf Dieter Schmid

[a]Institute of Biochemistry, Heinrich-Heine University Düsseldorf, Universitätsstr.1, 40225 Düsseldorf, Germany

[b]Cluster of Excellence on Plant Sciences, Heinrich-Heine University Düsseldorf, Universitätsstr.1, 40225 Düsseldorf, Germany

*Corresponding author:

Vlada B. Urlacher

Universitätsstr.1

40225 Düsseldorf

Germany

Phone: +49 211 13889

Fax: +49 211 81 13117

Email: vlada.urlacher@uni-duesseldorf.de

Abstract

The *Arabidopsis thaliana* gene encoding CYP71A16 is part of the gene cluster for the biosynthesis and modification of the triterpenoid marneral. Previous investigations of *A. thaliana* have revealed that CYP71A16 oxidizes marneral, while it also can accept marnerol as substrate. The aim of the present study was to investigate functional properties of CYP71A16 *in vitro*. For this purpose, heterologous expression of a N-terminally modified version of CYP71A16 was established in *Escherichia coli*, which yielded up to 50 $mg \cdot L^{-1}$ recombinant enzyme. The enzyme was purified and activity was reconstituted *in vitro* with different redox partners. A heterologous bacterial redox partner system consisting of the flavodoxin YkuN from *Bacillus subtilis* and the flavodoxin reductase Fpr from *E. coli* clearly outperformed the cytochrome P450 reductase ATR2 from *A. thaliana* in supporting the CYP71A16-mediated hydroxylation of marnerol. Substrate binding experiments with CYP71A16 revealed a dissociation constant K_D of 225 µM for marnerol. CYP71A16 hydroxylated marnerol to 23-hydroxmarnerol with a K_M of 142 µM and a k_{cat} of 3.9 min^{-1}. Furthermore, GC/MS analysis revealed an as of yet unidentified overoxidation product of this *in vitro* reaction.

Keywords: CYP71A16, *E. coli*, plant triterpenoid, marnerol, ATR2, heterologous expression

[1] Abbreviations used: P450, Cytochrome P450 monooxygenase; CPR, Cytochrome P450 reductase; LB, Lysogeny broth (medium); TB, Terrific broth (medium); IPTG, isopropyl-β-D-thiogalactopyranoside; GC/MS, Gas chromatography coupled with mass spectrometry; HPLC, high performance liquid chromatography; NADPH, reduced nicotinamide adenine dinucleotide phosphate; $NADP^+$, nicotinamide adenine dinucleotide phosphate; SDS-PAGE, sodium dodecyl sulfate-polyacrylamide gel electrophoresis; GDH, glucose dehydrogenase; Tris, tris(hydroxymethyl)aminomethane; EDTA, ethylenediaminetetraacetic acid; PMSF, phenylmethylsulfonyl fluoride ; Ni-NTA, nickel-nitrilotriacetic acid; IMAC, immobilized metal ion affinity chromatography.

1. Introduction

Cytochrome P450 monooxygenases (P450s) are heme *b* containing enzymes. They catalyze the reductive scission of molecular oxygen: herein one atom of molecular oxygen is introduced into the substrate, whereas the second oxygen atom is reduced to water. P450s are widely distributed in nature and accept a broad range of substrates including terpenoids, antibiotics, fatty acids, vitamins, alkanes and many other substance classes [1,2]. In plants, P450s are typically bound to the membrane via their N-terminal membrane-anchoring region and interact with a membrane-anchored cytochrome P450 reductase (CPR) that supplies the necessary electrons derived from the nicotinamide adenine dinucleotide cofactors. Most plant P450s are involved in the synthesis and diversification of natural products, which often play an important role in plant development and defence, or can act as medicines [3]. Plant P450s are responsible for among others the modification of terpenoids, including triterpenoids. Triterpenoids are thought to influence plant growth and development [4], as well as defence processes in plants [5]. Furthermore, triterpenoids are known for a number of health beneficial effects, including chemo-preventive and chemo-therapeutic properties [6], which make them attractive molecules for pharmaceutical purposes. Structurally, triterpenoids are C30 molecules derived from repetitive fusions of isoprenoid units. The precursor squalene is oxidized to 2,3-oxidosqualene that is in turn cyclized by specific triterpene synthases/cyclases to furnish different triterpenoid scaffolds that serve as substrates for various P450s for further modification [7].

CYP71A16 from *Arabidopsis thaliana* is involved in the marneral synthesis and modification pathway [8]. Marneral has been proposed as an intermediate in the biosynthesis of the special group of triterpenoids in Iridaceae; the so-called iridals [9,10]. Iridals have been shown to exhibit neuroprotective properties [11], cytotoxic effects on human cancer cell lines [12] and antitrypanosomal activity [13]. Remarkably, the gene encoding CYP71A16 is localized in a gene cluster together with the genes encoding marneral synthase MRN1 and CYP705A12 of unknown function [8]. Such gene organization is not typical for eukaryotes, but has been reported for several plants [14–16].

Regarding the physiological function of marneral, *A. thaliana* knock-out mutants that lack the MRN1 gene, showed delayed growth and build round-shaped leaves [4], whereas overexpression of MRN1, either alone or together with the gene encoding CYP71A16 resulted in abnormal dwarfed phenotypes of *A. thaliana* [8]. The involvement of CYP71A16 in the oxidation of marneral and its derivative marnerol has been demonstrated *in planta* as well as in recombinant *S. cerevisiae* [8,17], but the enzyme has not been characterized in detail. Plants overexpressing MRN1 and CYP71A16 produced seven new compounds, four of which were identified as isomers of hydroxylated desaturated marnerol [8]. Interestingly, *S. cerevisiae* expressing MRN1, CYP71A16 and the cytochrome P450 reductase ATR2 produced mainly hydroxymarnerol, a small amount hydroxymarneral, and very minor unidentified side-chain oxygenated marnerol derivatives [17].

In the present study, we aimed at CYP71A16 expression in *E. coli* and further protein purification to conduct its characterization *in vitro*. Suitable autologous and heterologous redox partners were identified and compared regarding their capacity to support CYP71A16 activity *in vitro*. Substrate binding studies were performed and the kinetic constants were determined for the CYP71A16-mediated conversion of marnerol to its hydroxylated derivative.

2. Materials and methods

2.1 Chemicals, vectors, and bacterial strains

The *E. coli* strain DH5α was purchased from Invitrogen (Karlsruhe, Germany). The expression vector pET-22b(+) was purchased from Novagen/EMD Millipore (Darmstadt, Germany). The *E. coli* expression strain C43 (DE3) was from Lucigen Corporation (Middleton, WI, USA). Phusion DNA Polymerase was obtained from Thermo Fisher Scientific (Schwerte, Germany) and oligonucleotides were purchased from MWG Eurofins Genomics (Ebersberg, Germany).

2.2 Cloning procedures

The gene encoding CYP71A16 was codon-optimized for expression in *E. coli*, and synthesized by MWG Eurofins Genomics (Ebersberg, Germany, see Supplementary Fig. S1). The putative transmembrane domain was identified using the TMHMM version 2.0 software (available at http://www.cbs.dtu.dk/services/TMHMM/). A number of CYP71A16 versions with modified N-terminal sequences and one construct with an additional C-terminal His_6-tag were constructed in polymerase chain reactions (PCRs) using the Phusion DNA polymerase under the following conditions: 98°C for 30 s; 30 cycles of 98°C for 5 s, 72°C for 25 s; and finally 72°C for 5 min. The modifications were introduced via primers 1 - 5 shown in Supplementary Table S1. The different gene versions were cloned into the pET-22b(+) vector.

The genes encoding the cytochrome P450 reductase ATR2 from the *A. thaliana* ecotypes Landsberg *erecta,* L-ATR2 (GenBank X66017.1) [18] and Columbia, C-ATR2 (GenBank NM_119167.4) [19] were codon-optimized for the expression in *E. coli* and *S. cerevisiae*, respectively (GenScript, Piscataway, USA and MWG Eurofins Genomics, Ebersberg, Germany). The genes were amplified by PCR using the Phusion DNA polymerase under the following conditions: 98°C for 30 s; 30 cycles of 98°C for 5 s and 72°C for 45 s; and finally 72°C for 5 min. For the N-terminal deletion of the initial 74 amino acids and the simultaneous introduction of an N-terminal His_6-tag, primers 6 and 7 were used for C-ATR2, whereas primers 8 and 9 were used for L-ATR2. For cloning purposes, the recognition sites for the endonucleases *Nde*I and *Hind*III were included in the corresponding primers. The modified genes were subsequently cloned into the pET-22b(+) vector to form the corresponding pET-22b(+)-*ATR2* constructs.

2.3 Expression and purification of the target proteins

CYP71A16

For the expression of CYP71A16, *E. coli* C43 (DE3) cells were transformed with the pET-22b(+)-*CYP71A16* constructs, carrying different modifications of this gene. 5 mL Lysogeny

Broth (LB) medium supplemented with ampicillin (100 µg·mL^{-1}) were inoculated either with a single colony from an LB agar plate or from cryo-preserved strain stocks, and cultivated overnight at 37°C and 180 rpm. For expression optimization studies, 100 mL Terrific Broth (TB) medium (in 500 mL Erlenmeyer flasks) were typically used, whereas large scale expressions were performed in 400 mL TB medium (in 2000 mL Erlenmeyer flasks). In all cases, medium was inoculated with pre-cultures to an optical density OD_{600} of 0.05. Cultures were then incubated at 37°C and 180 rpm to an OD_{600} of 0.6 - 0.8 and gene expression was induced by the addition of IPTG (0.5 mM final concentration). In addition, the cultures were supplemented with 5'-aminolevulinic acid (0.5 mM final concentration) and expression was performed at 20°C, while shaking at 120 rpm for 96 hours, unless stated otherwise. *E. coli* cells were harvested by centrifugation and resuspended in 50 mM Tris-HCl, pH 7.5 buffer containing 20% (v/v) glycerol, 1 mM EDTA and 0.2% (v/v) Triton X-100 (in case of further purification usually 50 mM Tris-HCl, pH 7.5 buffer containing 20 mM imidazole, and 500 mM KCl was used). Next, 0.3 mg lysozyme per mg cell wet weight and PMSF (0.1 mM final concentration) were added and cells were disrupted by sonication. Hereafter, the cell debris was removed by centrifugation (27216 g, 4°C, 20 min).

For purification of CYP71A16, a self-packed 3 mL Ni-NTA agarose (Qiagen, Hilden, Germany) column was used. The column was equilibrated with 10 column volumes (CV) of buffer 50 mM Tris HCl, pH 7.5, 500 mM KCl, containing 20 mM imidazole before the protein sample in the same buffer solution was applied. The column was then washed with 5 CV of the buffer including 20 mM imidazole. Next, non-specifically bound proteins were washed from the column with 5 - 10 CV of the same buffer containing 40 mM imidazole, whereas elution of the P450 was accomplished with 4 - 5 mL of buffer containing 250 mM imidazole. The IMAC-purified protein samples were concentrated with Vivaspin® Turbo 15 Turbo 30K MWCO concentrators and desalted using Econo-Pac® 10DG Desalting (Bio-Rad) with 50 mM potassium phosphate buffer pH 7.5 containing 20% (v/v) glycerol.

ATR2

For the expression of ATR2, *E. coli* C43 (DE3) cells were transformed with the pET-22b(+)-*ATR2* based constructs. Expression was performed as described for CYP71A16 with the exception that expression was induced with IPTG at a final concentration of 1 mM under supplementation of riboflavin (5 $\mu g \cdot L^{-1}$ final concentration) as described in [20]. Expression was carried out at 20°C and 120 rpm for 20 - 24 hours. Afterwards, *E. coli* cells were harvested and suspended in 100 mM Tris-HCl, pH 8.2 buffer containing 100 mM KCl, 2 mM EDTA, and 0.1 mM PMSF; in case of purification the same buffer lacking EDTA was used, similar as described in [20]. Cells were disrupted by sonication and the cell debris was removed by centrifugation (27216 g, 4°C, 20 min). ATR2 was purified from the supernatant using a 5 mL HisTrap FF column (GE Healthcare, Little Chalfont, UK). ATR2 was eluted with a linear gradient of 10 mM to 500 mM imidazole in buffer consisting of 100 mM Tris-HCl, pH 8.2 and 100 mM KCl. After purification and concentration using Vivaspin® Turbo 15 Turbo 50K MWCO concentrators, the purified protein was desalted using PD MidiTrap G25 columns (GE Healthcare) using 50 mM potassium phosphate buffer, pH 7.5 as eluent. For the determination of the extinction coefficients for ATR2 at 381 nm and 453 nm, the protein was further purified by size exclusion chromatography. For this purpose, the purified protein solution was diluted to 5 $mg \cdot mL^{-1}$ in 50 mM potassium phosphate buffer, pH 7.5 supplemented with 100 mM KCl, and filtered through a 0.45 µm filter. The protein solution was then applied to a Superdex 200 Increase 10/300 GL column (GE Healthcare), and eluted with 50 mM potassium phosphate buffer, pH 7.5 supplemented with 100 mM KCl. Protein elution was monitored by measuring the absorbance at wavelengths 220 nm, 383 nm and 458 nm. Finally, the ATR2 containing fractions were pooled, concentrated and desalted using a PD MidiTrap G25 column with 50 mM potassium phosphate buffer, pH 7.5 as elution buffer and stored at -20°C until use.

YkuN and Fpr

The vectors encoding the genes for the redox partners YkuN and Fpr as well as procedures for enzyme expression and purification have been described elsewhere [21,22]. In addition, the YkuN-Fpr fusion protein YR-P5 [Bakkes PJ, personal communication] was used as alternative redox partner system for CYP71A16.

GDH

The gene encoding the glucose dehydrogenase (GDH, GenBank D10626) from *Bacillus megaterium* in pET-22b(+) was expressed as described previously [23]. Optionally a two-step procedure for the purification of GDH from *E. coli* lysate was performed by using salt precipitation and heat denaturation [24]. To this end, the cells were resuspended in 50 mM potassium phosphate buffer pH 7.5 supplemented with 2 M NaCl and disrupted by sonication. Then, the lysate was cleared by centrifugation (40000 g, 4°C, 25 min) and the supernatant was carefully removed and incubated at 60°C for 20 min. Precipitated proteins were removed by centrifugation at 40000 g, 4°C for 25 min and the soluble fraction containing the purified GDH was stored at -20°C until use.

2.4 Determination of protein concentration and enzyme assays

Concentrations of CYP71A16 variants were measured spectrophotometrically as described previously with the use of the extinction coefficient $\varepsilon_{450\text{-}490}$= 91 $mM^{-1}\cdot cm^{-1}$ [25]. Concentrations of YkuN and Fpr were determined with the use of the published extinction coefficients for YkuN of ε_{461}=10.01 $mM^{-1}\cdot cm^{-1}$ [26,27] and for Fpr of ε_{456}= 7.1 $mM^{-1}\cdot cm^{-1}$ [28].

For determination of ATR2 concentrations the extinction coefficients ε_{453}= 13.7 $mM^{-1}\cdot cm^{-1}$ and ε_{381}= 12.6 $mM^{-1}\cdot cm^{-1}$ were used. The coefficients were determined by recording an absorbance spectrum (from 300 - 800 nm) of purified C-ATR2 after size-exclusion chromatography. The specific extinction coefficients were calculated by the Lambert-Beer law ($A=\varepsilon\cdot c\cdot d$); the protein concentration c was measured by an assay based on the Bradford method.

ATR2 activity was measured in a photometrical assay using cytochrome *c* as external electron acceptor. A standard reaction was performed in 1 mL volume and contained 300 mM potassium phosphate buffer, pH 7.7, 50 µM cytochrome *c* from equine heart (Calbiochem, Merck KGaA, Darmstadt, Germany) and cleared cell lysate or purified enzyme in an appropriate dilution. The reactions were started by addition of NADPH (100 µM final concentration). Reduction of cytochrome *c* was measured by monitoring the increase in absorbance at 550 nm for 2 minutes [29]. Activities were calculated using the combined extinction coefficient between oxidized and reduced cytochrome *c* of $\Delta\varepsilon$= 21 $mM^{-1} \cdot cm^{-1}$ [30].

The activity of GDH was determined in a photometric assay. A 1 mL reaction contained 50 mM potassium phosphate buffer, pH 7.5, 100 µM glucose and 100 µL of cell free extract or (partially) purified enzyme in an appropriate dilution. The reaction was started by the addition of $NADP^+$ (final concentration of 100 µM) and changes in absorbance at 340 nm (ε_{340}=6.22 $mM^{-1} \cdot cm^{-1}$) were recorded for 2 minutes.

Total protein concentrations were determined in an assay based on the Bradford method [31] using RotiQuant reagent (Carl Roth, Karlsruhe, Germany) and bovine serum albumin as protein standard.

2.5 Marnerol synthesis and purification

The *Saccharomyces cerevisiae* GIL-77 pYES/DEST-52 *MRN1* strain [8] was kindly provided by Prof. Anne Osbourn (Department of Metabolic Biology, John Innes Centre, Norwich, UK) and marnerol was produced as described previously [32]. Marnerol was purified from the crude yeast extract by semipreparative HPLC (Prominence instrument, Shimadzu, Tokyo, Japan) using a Eurospher II 100-10-C18 (10.0 µm, 300 x 8 mm, Bischoff, Leonberg, Germany) column. The column temperature was 30°C and the flow rate 5 $mL \cdot min^{-1}$. A solvent gradient was applied using solvent A which consisted of water with 0.1% (v/v) formic acid and solvent B which consisted of 100% methanol . The gradient was started from 85% B and increased to 100% B in 19 minutes and then held for 1 minute. The concentration of B was then lowered to 85% again and was hold for 5 minutes. Marnerol absorbance was

detected at wavelengths of 190 nm and 210 nm, the marnerol peak at a retention time of 22.66 minutes was collected. A total of 9.1 mg marnerol (purity >98% by GC/MS; HPLC) was obtained from 3 L yeast culture.

2.6 *In vitro* conversion of marnerol by CYP71A16

A standard reaction was performed with purified enzymes in 250 µL volume in 2 mL plastic reaction tubes. Each reaction, unless stated otherwise, contained 2 µM P450 and 8 µM each of redox partners; YkuN and Fpr, or ATR2. NADPH (400 µM) was regenerated by adding GDH (12 $U \cdot mL^{-1}$) in the presence of 100 mM glucose. For removal of hydrogen peroxide catalase from bovine liver (~620 $U \cdot mL^{-1}$, Sigma-Aldrich, St. Louis, MO, USA) was added. The substrate (100 µM final concentration) was added from a 10 mM stock solution in ethanol. The reactions were performed in 50 mM potassium phosphate buffer, pH 7.5 containing 0.12% (v/v) Triton X-100 (or alternatively 0.5% (w/v) fos-choline 14, 0.5% (w/v) L-α-phosphatidylcholine, or 0.5% (v/v) igepal CO-520) and were initiated by the addition of NADPH to a final concentration of 200 µM. The samples were incubated at 25°C in an overhead shaker with moderate rotation of 10 rpm for 20 hours, or in a thermoshaker for 20 hours with vigorous shaking at 450 rpm. Substrate and products were extracted twice with 250 µL ethyl acetate. The organic phase was evaporated and the residue was suspended in 200 µL 25% (v/v) methanol. Triton X-100 was removed via Stage Tip extraction using pipette tips packed with five layers of a C18 material (Empore™ C18 47 mm Extraction Disc, model 2215, 3M, St Paul, MN, USA) [33]. Prior to use, the membranes were activated with 100 µL of 100% methanol and, equilibrated with 100 µL of 25% (v/v) methanol. After each step a centrifugation step at 4900 g was performed. Hereafter, the sample was applied and the material was washed using 50% (v/v) and 75% (v/v) methanol. The bound substrate and products were then eluted with 100% (v/v) methanol. After sample application centrifugation steps were performed at 1700 g. Methanol was evaporated under reduced pressure prior to derivatization using 30 µl *N*,*O*-Bis(trimethylsilyl)trifluoroacetamide (BSTFA) with 1% (v/v) trimethylchlorosilane typically at 80°C for 30 min. Samples were then subjected to GC/MS analysis.

For determination of kinetic parameters, reactions were set up as described above with the exception that concentrations of marnerol ranged from 10 - 500 µM (final concentration of ethanol in each reaction was 1% (v/v)). The incubation was performed in a thermoshaker at 25°C with shaking at 450 rpm. After 2.5 min, to a time point at which product formation was linear, samples were extracted and derivatized as described above, followed by GC/MS analysis. Conversion was calculated by setting peak areas of substrate plus product as 100%. The corresponding k_{cat} and K_M values were calculated by plotting the rate of product formation (nmol product per min) against the different substrate concentrations. The results were fitted to the Michaelis-Menten equation $V_0 = V_{max} \cdot [S] / (K_M + [S])$, where *[S]* is the substrate concentration, V_0 the initial reaction velocity and V_{max} the maximum reaction velocity, by using OriginPro 9.0G software (OriginLab Corporation, Northampton, MA, USA). The reactions were performed in triplicates.

For determination of NADPH oxidation rates and coupling efficiency (a molar ratio of NADPH consumed to the product formed) the standard reaction set up was applied, however without cofactor regeneration. NADPH (1 mM) was added to start reaction, and the absorption at 340 nm was followed. The NADPH oxidation rate was calculated using ε=6.22 $mM^{-1}cm^{-1}$. After all NADPH was completely consumed, the residual substrate and products were extracted as described above and analyzed by GC/MS to determine the coupling efficiency.

2.7 Product analysis by GC/MS analysis

Trimethylsilylated samples were analyzed on a GC/MS-QP2010 (Shimadzu) with a FS-Supreme-5 column (30 m x 0.25 mm x 0.25 µm, CS-Chromatographie Service GmbH, Langerwehe, Germany). Helium was used as carrier gas. The column oven temperature was set to 250°C and the injection temperature was 300°C. The initial oven temperature was held for 2 minutes at 250°C, then ramped to 320°C with a rate of 5°C/ min, after which the temperature was kept at 320°C for 3 minutes.

2.8 Substrate binding studies

Spin-state shifts were determined with a Lambda 35 dual-beam spectrophotometer (PerkinElmer, Waltham, MA, USA) equipped with two tandem quartz cuvettes (Hellma, Müllheim, Germany) at 22 °C. One chamber of each cuvette was filled with 800 µL solution containing 1 µM P450 in 50 mM potassium phosphate buffer, pH 7.5, whereas the second chamber was filled with the buffer only. Next, the substrate was added to the chamber with P450 in the sample cuvette, as well as to the buffer chamber in the reference cuvette. All substrates were solved in 100% ethanol except for agatholal and valencene which were both solved in 100% dimethyl sulfoxide. Absorbance spectra were recorded in the range of 330 - 550 nm. The absorbance difference was plotted against the concentration of the substrate and the dissociation constant (K_D) was calculated by fitting the results to the following equation $\Delta A = \Delta A_{max} \cdot [S] / [K_D + [S]$, where ΔA is the absorbance difference between peak maximum and minimum; ΔA_{max} is the maximum difference in absorbance; $[S]$ is the substrate concentration, using OriginPro 9.0G software (OriginLab Corporation).

3. Results

3.1 Expression and purification of CYP71A16

Typically, plant P450s are membrane-bound via their N-terminus, which makes their expression in bacterial hosts difficult. To improve expression, N-terminally truncated and/or modified gene variants are frequently created to produce increased amounts of functional protein, as shown for *e.g.* human CYP4F11 [34], *Sorghum bicolor* tyrosine N-hydroxylase CYP79A1 [35] and the spearmint limonene-6-hydroxylase CYP71D18 [36]. Here, we cloned and expressed the native sequence of CYP71A16 as well as two variants thereof carrying a modified N-terminus (Table 1) in *E. coli*.

The putative (trans)membrane region of CYP71A16 was identified using the TMHMM software v. 2.0. Based on this analysis, the amino acids EMMILIS were replaced by the modified hydrophobic amino acid sequence ALLLAVF which originates from the bovine CYP17A1 [37], thus generating CYP71A16bov. In the second variant, designated as CYP71A16rab, the modified sequence AKKTSSKGK of the rabbit CYP2C3 containing several polar of charged amino acids [38] was introduced instead of the predicted membrane region (the first 24 amino acids). The highest expression yields were obtained with the variant CYP71A16rab as evidenced by the characteristic peak at 450 nm in the CO-difference spectrum. After 45 h of expression ~2 $mg \cdot L^{-1}$ CYP71A16bov and ~5 $mg \cdot L^{-1}$ CYP71A16rab were detected, whereas upon expression of the native gene, no spectral changes were observed. Upon increasing the expression time from 45 h to 96 h, an up to 10-fold increase in the CYP71A16rab level was achieved, yielding ~50 mg CYP71A16rab per 1 liter of culture broth. As shown in Fig. 1A, the corresponding CO-difference spectrum exhibits the characteristic absorbance maximum at 450 nm.

To allow easy purification of CYP71A16rab, a hexahistidine (His_6)-tag was added to the C-terminus during cloning, and the corresponding protein was purified by immobilized metal ion affinity chromatography (IMAC) (Fig. 1B). The His_6-tagged CYP71A16rab has an expected Mw of ~55 kDa and could be partially purified with an approximate purity of up to

90% as estimated by SDS-PAGE analysis (Fig. 1B). The total enzyme recovery after purification calculated based on the CO-difference spectrum was ~80%.

3.2 Expression and purification of the cytochrome P450 reductase ATR2

As a possible redox partner for CYP71A16, the cytochrome P450 reductase (CPR) ATR2 from *A. thaliana* was tested first, as this CPR has been used as electron transfer partner of CYP71A16 for marnerol oxidation in recombinant *S. cerevisiae* [17]. Moreover, several ATR2 variants with partially truncated membrane anchor (N-terminus) have been successfully expressed in *E. coli* before [20,39]. We investigated two versions of ATR2. To this end, the genes encoding L-ATR2 from *A. thaliana* Landsberg *erecta* and C-ATR2 from *A. thaliana* Columbia (Supplementary Fig. S2 and S3), which differ in only 11 amino acids, were expressed in *E. coli* C43 (DE3). The structure of C-ATR has been recently published [40], according to that, some of the amino acids that differ in C- and L-ATR2 are located within the FAD binding domain. The initial 74 amino acids of L-ATR2 and C-ATR2 corresponding to the membrane anchor were deleted and a His_6-tag was introduced at the N-terminus. The activity of the ATR2 variants in the corresponding cleared cell lysates was determined using cytochrome *c* as the artificial electron acceptor (Fig. 2A).

L-ATR2 cleared cell lysates showed a similar activity to the negative control, whereas C-ATR2 cleared cell lysates clearly showed an activity above the background level suggesting functional expression of this variant. A specific activity of almost 1 $U \cdot mg^{-1}$ towards cytochrome *c* was measured. In line with this, SDS-PAGE analysis revealed an additional protein band of the expected Mw of 72 kDa in the lane with C-ATR2 lysate, whereas this band was absent in both the negative control and *E. coli* lysate after L-ATR2 expression (Fig. 2B). Thus, for further experiments, the reductase from the ecotype Col-0, C-ATR2, was used.

The recombinant C-ATR2 was purified with the help of the N-terminal His_6-Tag using IMAC. As demonstrated by SDS-PAGE analysis, the target protein with a corresponding Mw of 72 kDa accumulated after purification, while only few additional protein bands were

detected in the eluate (Fig. 3A). For further purification, size exclusion chromatography was performed (Supplementary Fig. S4), yielding purified C-ATR2 (Fig. 3A). For calculation of the extinction coefficients, a spectrum in a range of 300 - 800 nm was recorded (Fig. 3B). The spectrum possesses two absorption maxima, which is typical for diflavin reductases; one peak at 453 nm and another one at 381 nm. The extinction coefficients were determined to be ε_{453}= 13.7 $mM^{-1}\cdot cm^{-1}$ and ε_{381}= 12.6 $mM^{-1}\cdot cm^{-1}$.

3.3 Reconstitution of CYP71A16rab activity *in vitro* with different redox partners

The substrates for CYP71A16, marneral and marnerol are not commercially available. Therefore, marnerol was produced in a recombinant *S. cerevisiae* strain according to Kushiro and coworkers [32] and isolated from the crude yeast extract. Marnerol was purified using semi-preparative HPLC and then applied as substrate to investigate CYP71A16rab activity *in vitro*. Reaction products were analyzed by GC/MS. As mentioned above, initial experiments were conducted with C-ATR2 from *A. thaliana*, as this cytochrome P450 reductase is suggested to be an endogenous redox partner of CYP71A16. At a ratio P450:C-ATR2 of 1:1, only 1.3% of the substrate was oxidized, whereas at a ratio P450:C-ATR2 of 1:4, 7.8% of marnerol was oxidized. Given the modest conversion, alternative redox partners were considered. We tested a bacterial redox partner system consisting of the FAD-containing flavodoxin reductase Fpr from *E. coli* and the FMN-containing flavodoxin YkuN from *B. subtilis,* which were demonstrated previously to effectively support catalysis of several bacterial P450s [21,41]. In addition, a fused version of YkuN and Fpr created in our laboratory [Bakkes PJ, personal communication] was tested. In this fusion protein, YkuN is connected to the N-terminus of Fpr via a rigid $([E/L]PPPP)_5$ linker. Indeed, the Fpr/YkuN redox pair was able to transfer electrons from NADPH to CYP71A16rab, as Fpr/YkuN supported nearly 60% conversion of marnerol in 20 h (Fig. 4). The YkuN-Fpr fusion protein also supported CYP71A16rab activity, albeit somewhat less effective, achieving 45% conversion under the same conditions.

To investigate the possible reasons for different conversions achieved with three redox partner sets, we measured the NADPH oxidation rates and coupling efficiencies in each combination. Whereas the P450 systems supported by C-ATR2 and Fpr/YkuN redox pair demonstrated low coupling efficiencies of <1%, YkuN-Fpr fusion resulted in a slightly higher coupling of 1%. The NADPH oxidation rate of 29 min^{-1} measured with Fpr/YkuN was higher than with C-ATR2 (5.5 min^{-1}) and with the YkuN-Fpr fusion (11 min^{-1}). This can explain a higher conversion achieved with Fpr/YkuN under cofactor regeneration conditions.

Independent of the redox partners used, in all CYP71A16rab-catalyzed reactions the marnerol peak was reduced and a new peak appeared with a retention time of 12.6 minutes (for example Fig. 5), which corresponds to the expected product 23-hydroxymarnerol. The product 23-hydroxymarnerol was identified by comparison with the fragmentation data reported previously [17] and is characterized by a molecular ion peak of m/z = 588 (Supplementary Fig. S6).

It is important to mention that marnerol was only converted to the product 23-hydroxymarnerol by CYP71A16 when 0.12% (v/v) Triton X-100 was present in the reaction mixture. However, for GC/MS compatibility, this nonionic detergent had to be removed, which was effectively accomplished by solid phase extraction performed with Stage-Tips. In addition, the effect of other detergents on marnerol conversion was tested. Remarkably, in the presence of 0.5% (w/v) fos-choline 14, or 0.5% (w/v) L-α-phosphatidylcholine, 23-hydroxymarnerol was not detected even after 20 h of conversion. In case of 0.5% (v/v) igepal CO-520, impurities appeared on the GC chromatograms that had the same retention times as the product. Thus, Triton X-100 was the most suitable detergent for this application and was used in further experiments.

3.4 *In vitro* characterization of CYP71A16rab

Since the Fpr/YkuN redox pair proved to be the best at supporting CYP71A16rab activity *in vitro*, this system was used in all subsequent experiments. Next, the influence of the

incubation conditions as well as the amount of P450 on marnerol conversion was investigated. Using an overhead shaker (10 rpm), a marnerol conversion of ~60% was typically attained (Fig. 4), whereas without shaking only ~30% conversion was achieved. In contrast, using planar orbital shaking (450 rpm) in a thermoshaker, marnerol conversion was almost complete after 20 h. Therefore, the time-dependent conversion of marnerol was studied under latter conditions (Fig. 6A).

Marnerol was consumed almost completely (98.5%) after 180 min in the reaction catalyzed by 2 µM CYP71A16rab in the presence of a fourfold excess of the redox partner proteins, Fpr and YkuN (Fig. 6A). Under these conditions, already after 30 minutes of conversion, a second product appeared in addition to 23-hydroxymarnerol. This unidentified component might be a marnerol overoxidation product (Supplementary Fig. S7 and S8), which accumulated to almost 30% of the total product after 20 h. The characteristic molecular ion peak of this trimethylsilylated product at m/z 514 may indicate oxidation of one of the alcohol groups of 23-hydroxymarnerol to an aldehyde. In the presence of 1 µM P450 only ~60% of marnerol was converted after 20 h (Fig. 6A), while only minor amounts of the overoxidation product were observed (< 1%).

For measuring kinetic constants, marnerol concentrations in the range 0 - 600 µM were used (Fig. 6B). A K_M value of 142.1 ± 29.3 µM and k_{cat} of 3.9 min^{-1} were determined for the CYP71A16rab-catalyzed *in vitro* conversion of marnerol.

3.5 Substrate binding studies

In addition to the kinetic constants, the substrate dissociation constant K_D for marnerol was determined (Fig. 7). Marnerol induced a Type I-binding spectrum, which is typical for substrates. Absorbance changes induced by marnerol binding to CYP71A16rab were plotted against the different concentrations of marnerol (Fig. 7). Based on the fitted data a K_D value of 225 µM was obtained.

In addition to marnerol, a number of other substances were tested for binding to CYP71A16rab. These substances included the pentacyclic triterpenoids lupeol, taraxasterol and α-amyrin, as well as the tetracyclic triterpenoids cycloartenol, butyrospermol and the steroid ergosterol. Moreover the bicyclic diterpenoids, valencene and agatholal, which bear a more structural resemblance to marnerol, were tested. Nevertheless, none of these selected substances induced a spectral shift in CYP71A16rab.

4. Discussion

The marneral biosynthesis pathway plays a significant role in *A. thaliana* development. Studies on an *A. thaliana* marneral pathway knock-out mutant as well as on *A. thaliana* overexpressing either marneral cyclase alone or together with marnerol oxidase CYP71A16 demonstrated altered plant phenotypes [4,8]. The goal of the present work was to gain more insights into the functional properties of CYP71A16 from the marnerol pathway.

Here, for the first time, the functional properties of *A. thaliana* CYP71A16 were studied *in vitro*. For this purpose, the gene encoding CYP71A16 was expressed in *E. coli.* However, expression of the native wild-type gene proved difficult, as it is often the case when membrane-bound P450s are expressed in bacterial hosts. To enable functional heterologous expression of membrane-bound P450s in *E. coli*, different strategies have been developed [42,43]. We used a codon-optimized for *E. coli* gene variant of CYP71A16, in which the natural N-terminal membrane anchor was replaced by a modified N-terminal sequence derived from rabbit CYP2C3 [38], which resulted in up to ~50 $mg \cdot L^{-1}$ active monooxygenase. In this respect, similar N-terminal substitutions have been reported for successful expression of a variety of eukaryotic P450 genes in *E. coli* [44–49]. The CO-difference spectra revealed that CYP71A16rab exhibits the typical absorbance maximum at 450 nm (Fig. 1A), which is indicative of proper heme iron coordination. Subsequent introduction of His_6-tag allowed the easy one-step purification of CYP71A16rab with an estimated purity of ~90% and a high protein recovery of ~80% (Fig. 1B).

P450 activity depends on electron transfer protein(s) that deliver the necessary NAD(P)H-derived electrons to the heme iron. As potential autologous redox partner for CYP71A16, ATR2 from *A. thaliana* was chosen, which has been shown to support the activity of a variety of plant P450s [19,20,36,50]. For this purpose, two previously published ATR2 gene variants, *i.e.* one from the *A. thaliana* ecotype Columbia (C-ATR2) [19] and the other from *Landsberg erecta* (L-ATR2) [18], were cloned and compared. Whereas the codon optimized gene coding for C-ATR2 could be expressed in *E. coli* after truncation of the N-

terminal membrane anchor, the same modifications did not enable expression of active L-ATR2. Recently, Castillo and coworkers suggested that the differences in the amino acid sequences between L-ATR2 and C-ATR2 variant, *i.e.* 11 amino acids in total, was due to the manual splicing technology available in 1992, and therefore the published sequence for L-ATR2 might be incorrect [17]. The failure to express functional L-ATR2 in *E. coli* appears to be consistent with this notion.

Importantly, the truncated purified C-ATR2 was able to support CYP71A16rab catalysis, suggesting that ATR2 might be a physiological redox partner of *A. thaliana* CYP71A16. However, since *A. thaliana* possesses another CPR gene as well as an additional putative CPR gene [18,51] it cannot be excluded that for instance the second CPR ATR1 is the natural redox partner of CYP71A16. The performance of C-ATR2 in supporting *in vitro* catalysis by CYP71A16rab was rather modest (Fig. 4). In the set up used, both C-ATR2 and CYP71A16rab lack their natural N-terminal membrane anchoring sequence, which may affect their functionality and can explain a very low coupling efficiency observed in this reaction. In this respect it has been observed that truncated but membrane-bound plant P450 and CPR (with a non-polar N-terminus added) work more efficient than truncated but likely soluble forms of these proteins (with a polar N-terminus added) in the production of oxygenated taxol precursors in *E. coli* [52]. In *A. thaliana*, ATR2 and CYP71A16 are membrane-localized proteins and thus their activity might be influenced by the lipid surrounding [53]. In this respect it is worth to mention that the activity of CYP71A16rab *in vitro* required the presence of Triton X-100. It is known that detergents can mimic biomembranes to some extent [54]. Alternatively, Triton X-100 may have improved the availability of the hydrophobic substrate marnerol for CYP71A16 catalysis as this compound has limited solubility in aqueous solutions.

Substitution of C-ATR2 by surrogate redox partners, Fpr/YkuN or a fused derivative thereof improved marnerol conversion (Fig. 4), probably because of higher NADPH consumption rates as compared with C-ATR2. This is an obvious advantage under cofactor regeneration conditions. Thus, this bacterial redox pair exhibits functional promiscuity, both

as separate enzymes or as artificial diflavin reductase, as they are able to support monooxygenase activity of P450s not only from bacterial and mammalian origin [41,55, Bakkes PJ, personal communication], but also from plant (Fig. 4). The substrate marnerol was shown to readily bind to CYP71A16rab, exhibiting a K_D of 225 µM, whereas steady-state kinetic studies of marnerol oxidation revealed a K_M value of 142.1 µM and a k_{cat} of 3.9 min^{-1}. Limited information on the kinetic constants of plant P450s for the oxidation of triterpenoids is currently available. For instance, in case of the oxidation of the phytosterols campesterol and campestanol by CYP90B1, K_M values were in the range of 0.35 – 3 µM, while k_{cat} values were 5.2 and 0.016 min^{-1}, respectively [56].

In addition to marnerol, other triterpenoid compounds were tested as potential substrates for CYP71A16rab. However, none of these compounds was able to bind to CYP71A16rab, which may indicate a narrow substrate spectrum of CYP71A16. However, it would be, interesting to investigate in the following work if these or any other substrates can be converted by this plant P450. Independent of the redox partner(s) used, 23-hydroxymarnerol was the main product formed by CYP71A16rab upon conversion of marnerol (Fig. 5). These data are consistent with *in vivo* observations for recombinant *S. cerevisiae* expressing marnerol synthase and CYP71A16 [17]. In our *in vitro* set up a further oxidation product of 23-hydroxymarnerol with a characteristic molecular ion of m/z 514 (after silylation) was detected, which indicates that *in vitro* one of the alcohol groups at position 3 or 23 was oxidized to an aldehyde if a high concentration of CYP71A16rab was used. NMR analyses will be performed in future to verify the structure of this compound.

5. Conclusion

Heterologous expression of a modified CYP71A16 gene was performed in *E. coli* producing functional CYP71A16rab at a high level. The enzyme was IMAC purified with high protein recovery and purity. CYP71A16rab activity was successfully reconstituted *in vitro* and required the presence of Triton X-100. Suitable redox partner(s) for productive electron

supply to CYP71A16rab were identified, with superior performance of the bacterial Fpr/YkuN system. GC/MS analysis confirmed that CYP71A16rab converts the natural triterpenoid substrate marnerol to the main product 23-hydroxymarnerol, which is in line with its proposed natural function. As CYP71A16 catalyzes an early oxidation step in the iridal biosynthesis, it has relevance for the synthesis and modification of this type of natural compounds; however its activity should be improved using protein engineering methods.

Competing interests

No competing interests are declared.

Author contributions

SK-F designed and conducted the experiments on expression and purification of CYP71A16 variants, *in vitro* reaction and determination of kinetic and dissociation constants, cloned, expressed and purified C-ATR2, evaluated the results and drafted the manuscript. OM helped in research design and data analysis. ER helped in marnerol purification using HPLC and revised the manuscript. ND performed experiments on determination of coupling efficiency and NADPH oxidation rates. PJB cloned the YkuN-Fpr fusion and revised the manuscript. VBU gave advices in the research work, helped in drafting the manuscript, and revised the manuscript. All authors read and approved the manuscript.

Funding

This work was supported by the Deutsche Forschungsgemeinschaft through the Cluster of Excellence on Plant Sciences (CEPLAS) [Project Reference Number: EXC 1028].

Acknowledgements

Prof. Anne Osbourn is gratefully acknowledged for providing the marnerol producing *S. cerevisiae* strain GIL77 pYES/DEST-52 *MRN1*. We would also thank Dr. Anita Loeschcke, Dr. Thomas Drepper and Prof. Karl-Erich Jaeger for providing the codon-optimized gene

encoding CYP71A16. We would also like to thank P.M. Ndjimi for cloning of L-ATR2 and S. Biemann and A. Worsch for providing YkuN and Fpr.

References

[1] V.B. Urlacher, M. Girhard, Cytochrome P450 monooxygenases: an update on perspectives for synthetic application, Trends Biotechnol. 30 (2012) 26–36.

[2] R. Bernhardt, Cytochromes P450 as versatile biocatalysts, J. Biotechnol. 124 (2006) 128–145.

[3] M. Morant, S. Bak, B.L. Møller, D. Werck-Reichhart, Plant cytochromes P450: tools for pharmacology, plant protection and phytoremediation, Curr. Opin. Biotechnol. 14 (2003) 151–162.

[4] Y.S. Go, S.B. Lee, H.J. Kim, J. Kim, H.-Y. Park, J.-K. Kim, K. Shibata, T. Yokota, K. Ohyama, T. Muranaka, S. Arseniyadis, M.C. Suh, Identification of marneral synthase, which is critical for growth and development in Arabidopsis, Plant J. 72 (2012) 791–804.

[5] D.R. Phillips, J.M. Rasbery, B. Bartel, S.P.T. Matsuda, Biosynthetic diversity in plant triterpene cyclization, Curr. Opin. Plant. Biol. 9 (2006) 305–314.

[6] P. Dzubak, M. Hajduch, D. Vydra, A. Hustova, M. Kvasnica, D. Biedermann, L. Markova, M. Urban, J. Sarek, Pharmacological activities of natural triterpenoids and their therapeutic implications, Nat. Prod. Rep. 23 (2006) 394–411.

[7] R. Croteau, T.M. Kutchan, N.G. Lewis, Natural products (secondary metabolites). 24, in: Buchanan, B, B, W. Gruissem, Jones, R, L (Eds.), Biochemistry and molecular biology of plants, American Society of Plant Physiologists: Rockville, MD, USA, 2000, pp. 1250–1319.

[8] B. Field, A.-S. Fiston-Lavier, A. Kemen, K. Geisler, H. Quesneville, A.E. Osbourn, Formation of plant metabolic gene clusters within dynamic chromosomal regions, Proc. Natl. Acad. Sci. U S A 108 (2011) 16116–16121.

[9] Q. Xiong, W.K. Wilson, S.P.T. Matsuda, An Arabidopsis oxidosqualene cyclase catalyzes iridal skeleton formation by Grob fragmentation, Angew. Chem. Int. Ed. Engl. 45 (2006) 1285–1288.

[10] F.-J. Marner, Iridals and cycloiridals, products of an unusual squalene metabolism in sword lilies (*Iridaceae*), Curr. Org. Chem. 1 (1997) 153–186.

[11] C.-L. Zhang, Y. Wang, Y.-F. Liu, G. Ni, D. Liang, H. Luo, X.-Y. Song, W.-Q. Zhang, R.-Y. Chen, N.-H. Chen, D.-Q. Yu, Iridal-type triterpenoids with neuroprotective activities from *Iris tectorum*, J. Nat. Prod. 77 (2014) 411–415.

[12] R. Fang, P.J. Houghton, P.J. Hylands, Cytotoxic effects of compounds from *Iris tectorum* on human cancer cell lines, J. Ethnopharmacol. 118 (2008) 257–263.

[13] A.L. Pathiranage, J.M. Stubblefield, X. Zhou, J. Miao, A.L. Newsome, N. Dunlap, Antitrypanosomal activity of iridals from *Iris domestica*, Phytochem. Lett. 18 (2016) 44–50.

[14] X. Qi, S. Bakht, M. Leggett, C. Maxwell, R. Melton, A. Osbourn, A gene cluster for secondary metabolism in oat: implications for the evolution of metabolic diversity in plants, Proc. Natl. Acad. Sci. U S A 101 (2004) 8233–8238.

[15] K. Papadopoulou, R.E. Melton, M. Leggett, M.J. Daniels, A.E. Osbourn, Compromised disease resistance in saponin-deficient plants, Proc. Natl. Acad. Sci. U S A 96 (1999) 12923–12928.

[16] A. Krokida, C. Delis, K. Geisler, C. Garagounis, D. Tsikou, L.M. Peña-Rodríguez, D. Katsarou, B. Field, A.E. Osbourn, K.K. Papadopoulou, A metabolic gene cluster in *Lotus japonicus* discloses novel enzyme functions and products in triterpene biosynthesis, New Phytol. 200 (2013) 675–690.

[17] D.A. Castillo, M.D. Kolesnikova, S.P.T. Matsuda, An effective strategy for exploring unknown metabolic pathways by genome mining, J. Am. Chem. Soc. 135 (2013) 5885–5894.

[18] P. Urban, C. Mignotte, M. Kazmaier, F. Delorme, D. Pompon, Cloning, yeast expression, and characterization of the coupling of two distantly related *Arabidopsis thaliana* NADPH-cytochrome P450 reductases with P450 CYP73A5, J. Biol. Chem. 272 (1997) 19176–19186.

[19] M. Mizutani, D. Ohta, Two isoforms of NADPH:cytochrome P450 reductase in *Arabidopsis thaliana*. Gene structure, heterologous expression in insect cells, and differential regulation, Plant Physiol. 116 (1998) 357–367.

[20] J. Schückel, E.L. Rylott, G. Grogan, N.C. Bruce, A gene-fusion approach to enabling plant cytochromes p450 for biocatalysis, Chembiochem 13 (2012) 2758–2763.

[21] M. Girhard, T. Klaus, Y. Khatri, R. Bernhardt, V.B. Urlacher, Characterization of the versatile monooxygenase CYP109B1 from *Bacillus subtilis*, Appl. Microbiol. Biotechnol. 87 (2010) 595–607.

[22] P.J. Bakkes, S. Biemann, A. Bokel, M. Eickholt, M. Girhard, V.B. Urlacher, Design and improvement of artificial redox modules by molecular fusion of flavodoxin and flavodoxin reductase from *Escherichia coli*, Sci. Rep. 5 (2015) 12158.

[23] P. Le-Huu, T. Heidt, B. Claasen, S. Laschat, V.B. Urlacher, Chemo-, regio-, and stereoselective oxidation of the monocyclic diterpenoid β-cembrenediol by P450 BM3, ACS Catal. 5 (2015) 1772–1780.

[24] T. Nagao, T. Mitamura, X.H. Wang, S. Negoro, T. Yomo, I. Urabe, H. Okada, Cloning, nucleotide sequences, and enzymatic properties of glucose dehydrogenase isozymes from *Bacillus megaterium* IAM1030, J. Bacteriol. 174 (1992) 5013–5020.

[25] T. Omura, R. Sato, The carbon monoxide-binding pigment of liver microsomes. II. Solubilization, purification, and properties, J. Biol. Chem. 239 (1964) 2379–2385.

[26] Z.-Q. Wang, R.J. Lawson, M.R. Buddha, C.-C. Wei, B.R. Crane, A.W. Munro, D.J. Stuehr, Bacterial flavodoxins support nitric oxide production by *Bacillus subtilis* nitric-oxide synthase, J. Biol. Chem. 282 (2007) 2196–2202.

[27] R.J. Lawson, C. von Wachenfeldt, I. Haq, J. Perkins, A.W. Munro, Expression and characterization of the two flavodoxin proteins of *Bacillus subtilis* , YkuN and YkuP: Biophysical properties and interactions with cytochrome P450 BioI, Biochemistry 43 (2004) 12390–12409.

[28] L. McIver, C. Leadbeater, D.J. Campopiano, R.L. Baxter, S.N. Daff, S.K. Chapman, A.W. Munro, Characterisation of flavodoxin NADP+ oxidoreductase and flavodoxin; key components of electron transfer in *Escherichia coli*, Eur. J. Biochem. 257 (1998) 577–585.

[29] J.L. Vermilion, M.J. Coon, Highly purified detergent-solubilized NADPH-cytochrome P-450 reductase from phenobarbital-induced rat liver microsomes, Biochem. Biophys. Res. Commun. 60 (1974) 1315–1322.

[30] B.F. van Gelder, E.C. Slater, The extinction coefficient of cytochrome c, Biochim. Biophys. Acta 58 (1962) 593–595.

[31] M.M. Bradford, A rapid and sensitive method for the quantitation of microgram quantities of protein utilizing the principle of protein-dye binding, Anal. Biochem. 72 (1976) 248–254.

[32] T. Kushiro, M. Shibuya, Y. Ebizuka, β-amyrin synthase–cloning of oxidosqualene cyclase that catalyzes the formation of the most popular triterpene among higher plants, Eur. J. Biochem. 256 (1998) 238–244.

[33] J. Rappsilber, Y. Ishihama, M. Mann, Stop and go extraction tips for matrix-assisted laser desorption/ionization, nanoelectrospray, and LC/MS sample pretreatment in proteomics, Anal. Chem. 75 (2003) 663–670.

[34] Z. Tang, S.G. Salamanca-Pinzón, Z.-L. Wu, Y. Xiao, F.P. Guengerich, Human cytochrome P450 4F11: Heterologous expression in bacteria, purification, and characterization of catalytic function, Arch. Biochem. Biophys. 494 (2010) 86–93.

[35] B.A. Halkier, H.L. Nielsen, B. Koch, B.L. Møller, Purification and characterization of recombinant cytochrome $P450_{TYR}$ expressed at high levels in *Escherichia coli*, Arch. Biochem. Biophys. 322 (1995) 369–377.

[36] C. Haudenschild, M. Schalk, F. Karp, R. Croteau, Functional expression of regiospecific cytochrome P450 limonene hydroxylases from mint (*Mentha* spp.) in *Escherichia coli* and *Saccharomyces cerevisiae*, Arch. Biochem. Biophys. 379 (2000) 127–136.

[37] H.J. Barnes, M.P. Arlotto, M.R. Waterman, Expression and enzymatic activity of recombinant cytochrome P450 17α-hydroxylase in *Escherichia coli*, Proc. Natl. Acad. Sci. U S A 88 (1991) 5597–5601.

[38] C. von Wachenfeldt, T.H. Richardson, J. Cosme, E.F. Johnson, Microsomal P450 2C3 is expressed as a soluble dimer in *Escherichia coli* following modification of its N-terminus, Arch. Biochem. Biophys. 339 (1997) 107–114.

[39] A.K. Hull, J.L. Celenza, Bacterial expression and purification of the Arabidopsis NADPH-cytochrome P450 reductase ATR2, Protein Expr. Purif. 18 (2000) 310–315.

[40] G. Niu, S. Zhao, L. Wang, W. Dong, L. Liu, Y. He, Structure of the *Arabidopsis thaliana* NADPH-cytochrome P450 reductase 2 (ATR2) provides insight into its function, FEBS J. 284 (2017) 754–765.

[41] C. von Bühler, P. Le-Huu, V.B. Urlacher, Cluster screening: an effective approach for probing the substrate space of uncharacterized cytochrome P450s, Chembiochem 14 (2013) 2189–2198.

[42] S. Zelasko, A. Palaria, A. Das, Optimizations to achieve high-level expression of cytochrome P450 proteins using *Escherichia coli* expression systems, Protein Expr. Purif. 92 (2013) 77–87.

[43] H. Duan, M.A. Schuler, Heterologous expression and strategies for encapsulation of membrane-localized plant P450s, Phytochem Rev 5 (2006) 507–523.

[44] D. Morrone, X. Chen, R.M. Coates, R.J. Peters, Characterization of the kaurene oxidase CYP701A3, a multifunctional cytochrome P450 from gibberellin biosynthesis, Biochem. J. 431 (2010) 337–344.

[45] Q. Wang, M.L. Hillwig, K. Okada, K. Yamazaki, Y. Wu, S. Swaminathan, H. Yamane, R.J. Peters, Characterization of CYP76M5-8 indicates metabolic plasticity within a plant biosynthetic gene cluster, J. Biol. Chem. 287 (2012) 6159–6168.

[46] Y. Wu, M.L. Hillwig, Q. Wang, R.J. Peters, Parsing a multifunctional biosynthetic gene cluster from rice: Biochemical characterization of CYP71Z6 & 7, FEBS Lett. 585 (2011) 3446–3451.

[47] Q. Wang, M.L. Hillwig, Y. Wu, R.J. Peters, CYP701A8: a rice *ent*-kaurene oxidase paralog diverted to more specialized diterpenoid metabolism, Plant Physiol. 158 (2012) 1418–1425.

[48] S. Swaminathan, D. Morrone, Q. Wang, D.B. Fulton, R.J. Peters, CYP76M7 is an *ent*-cassadiene C11α-hydroxylase defining a second multifunctional diterpenoid biosynthetic gene cluster in rice, Plant Cell 21 (2009) 3315–3325.

[49] C.D. Sohl, F.P. Guengerich, Kinetic analysis of the three-step steroid aromatase reaction of human cytochrome P450 19A1, J. Biol. Chem. 285 (2010) 17734–17743.

[50] Y. Miki, Y. Asano, Biosynthetic pathway for the cyanide-free production of phenylacetonitrile in *Escherichia coli* by utilizing plant cytochrome P450 79A2 and bacterial aldoxime dehydratase, Appl. Environ. Microbiol. 80 (2014) 6828–6836.

[51] J. Varadarajan, J. Guilleminot, C. Saint-Jore-Dupas, B. Piégu, M.-E. Chabouté, V. Gomord, R.C. Coolbaugh, M. Devic, V. Delorme, ATR3 encodes a diflavin reductase essential for Arabidopsis embryo development, New Phytol. 187 (2010) 67–82.

[52] B.W. Biggs, C.G. Lim, K. Sagliani, S. Shankar, G. Stephanopoulos, M. de Mey, P.K. Ajikumar, Overcoming heterologous protein interdependency to optimize P450-mediated taxol precursor synthesis in *Escherichia coli*, Proc. Natl. Acad. Sci. U S A 113 (2016) 3209–3214.

[53] S. Imaoka, Y. Imai, T. Shimada, Y. Funae, Role of phospholipids in reconstituted cytochrome P 450 3A form and mechanism of their activation of catalytic activity, Biochemistry 31 (1992) 6063–6069.

[54] A.M. Seddon, P. Curnow, P.J. Booth, Membrane proteins, lipids and detergents: not just a soap opera, Biochim. Biophys. Acta 1666 (2004) 105–117.

[55] A. Rühlmann, D. Antovic, T.J.J. Müller, V.B. Urlacher, Regioselective hydroxylation of stilbenes by engineered cytochrome P450 from *Thermobifida fusca* YX, Adv. Synth. Catal. 359 (2017) 984–994.

[56] S. Fujita, T. Ohnishi, B. Watanabe, T. Yokota, S. Takatsuto, S. Fujioka, S. Yoshida, K. Sakata, M. Mizutani, Arabidopsis CYP90B1 catalyses the early C-22 hydroxylation of C_{27}, C_{28} and C_{29} sterols, Plant J. 45 (2006) 765–774.

Tables

Table 1. N-terminal modifications (shown in bold) of the amino acid sequence of CYP71A16. The predicted transmembrane part in the native sequence is underlined.

Construct CYP71A16	Amino acid sequence	Used abbreviation
native sequence	MEMMILISLCLTTFLTILLFFKSLLKRPN	CYP71A16
$_{\Delta 1\text{-}7}$C17A	M**ALLLAVF**LCLTTFLTILLFFKSLLKRPN	CYP71A16bov
$_{\Delta 1\text{-}23}$C2C3	M**AKKTSSKGK**LKRPN	CYP71A16rab

Figure legends

Fig. 1. A) CO-difference spectrum of cleared *E. coli* cell lysate containing CYP71A16rab after 96 h expression. B) 12.5% SDS-PAGE analysis of purification of CYP71A16rab carrying C-terminal His_6-tag. 10 µg total protein per lane was applied. M: marker proteins with corresponding molecular weights given in kDa; L: cleared cell lysate; FT: flow-through; W1: wash 1 (20 mM imidazole); W2: wash 2 (40 mM imidazole), and E: eluate after desalting.

Fig. 2. Comparison of C-ATR and L-ATR activity and expression. A) Cytochrome *c* reduction activity of cleared *E. coli* cell lysates after expression of ATR2 variants from *A. thaliana* Columbia (C-ATR2) and Landsberg *erecta* (L-ATR2). Specific activities towards cytochrome *c* are given in $U \cdot mg^{-1}$. Data represent the average of duplicate expressions (the negative control – Neg - was performed as single expression experiment) and triplicate measurements of the cytochrome *c* activity. In case of Neg and L-ATR2 standard deviations were < 0.01 $U \cdot mg^{-1}$. B) 12.5% SDS-PAGE analysis of the cleared cell lysates after 20 h expression of C-ATR2 (C) and L-ATR2 (L). The negative control (Neg) represents the cleared cell lysate of *E. coli* strain with empty vector treated in an identical manner. M: marker proteins with indicated molecular weights in kDa.

Fig. 3. A) 12.5% SDS-PAGE analysis of purification of C-ATR2. 15 µg of total protein was applied in each lane. M: marker proteins with molecular weights indicated in kDa; L: cleared cell lysate; FT: IMAC flow-through: W1, wash 1 (without imidazole), W2: wash 2 (10 mM imidazole); E: IMAC (100 mM imidazole) eluate after desalting and SEC, eluate after size-exclusion chromatography (2 µg protein was applied). B) UV/Vis spectrum of purified C-ATR2 after size-exclusion chromatography showing characteristic absorbance maxima at 453 nm and 381 nm.

Fig. 4. CYP71A16rab catalyzed conversion of marnerol supported by different redox partners. Comparison of the redox partner systems YkuN and Fpr, YkuN-Fpr fusion, and C-ATR2. Marnerol conversion (%) is shown. Reactions were incubated at 25°C for 20 h in an overhead shaker. Mean values and standard deviations were calculated from three independent reactions.

Fig. 5. Chromatograms of the GC/MS analysis of marnerol conversions catalyzed by CYP71A16rab with Fpr/YkuN as redox partners (solid line) and a negative control without P450 (dashed line). Reactions were performed at 25°C in an overhead shaker for 20 hours. Samples were extracted with ethylacetate and removal of Triton X-100 was performed with Stage-Tips. Samples were derivatized with *N*,*O*-Bis(trimethylsilyl)trifluoroacetamide prior to GC/MS analysis. The asterisk indicates low amounts of residual Triton X-100.

Fig. 6. Marnerol conversion catalyzed by CYP71A16rab with YkuN and Fpr as redox partners. A) Time course of marnerol conversion. Marnerol was used at a final concentration of 100 µM and CYP71A16rab at concentrations of 1 µM and 2 µM, while redox partners were used in all cases in a fourfold molar excess. B) Determination of the reaction velocity (v) in nmol product per min based on 23-hydroxymarnerol formation. 2 µM P450 was used in the reactions with a fourfold molar excess of the redox partners Fpr/YkuN, while different marnerol concentrations (10 - 500 µM) were applied. Conversion reactions were stopped after 2.5 min. Error bars indicate standard deviations from three experiments. The data points are fitted to the equation described in materials and methods (correlation coefficient of determination $R^2 = 0.96$).

Fig. 7. Absorbance changes, induced by marnerol binding to CYP71A16rab, are plotted against the concentration of marnerol. The absorbance maximum was detected at 393 nm and the minimum at 429 nm. The data points are fitted to the equation described in materials and methods (correlation coefficient of determination $R^2 = 0.97$)

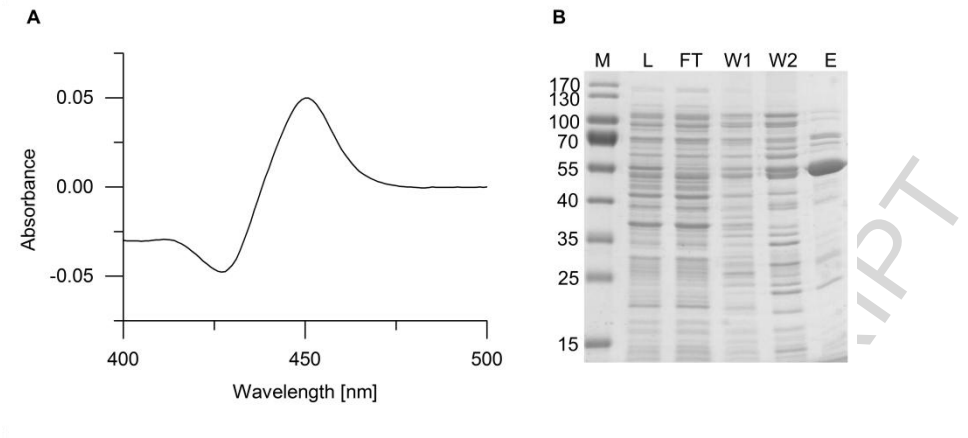

Figure 1

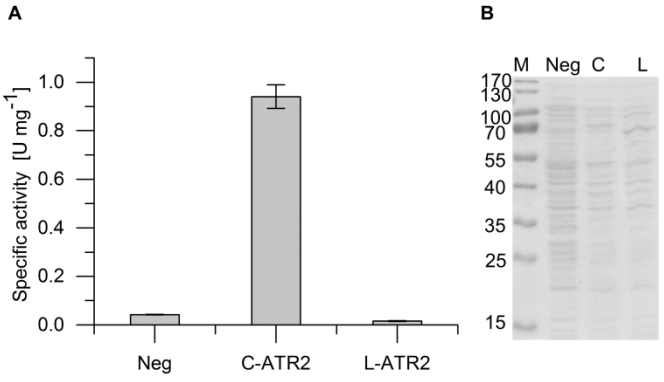

Figure 2

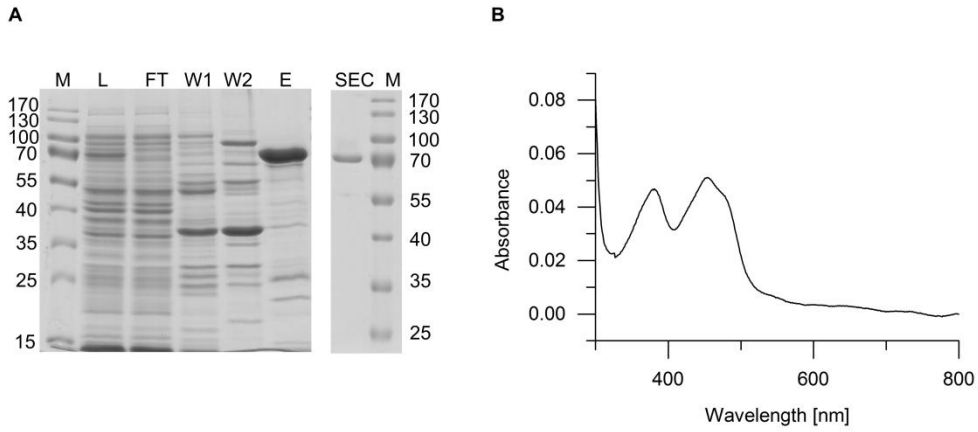

Figure 3

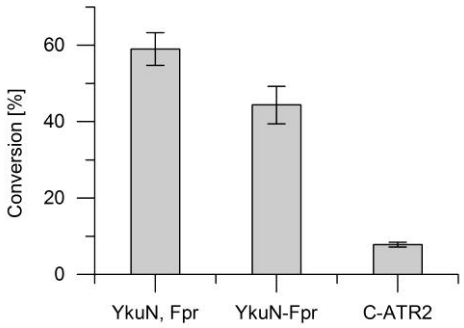

Figure 4

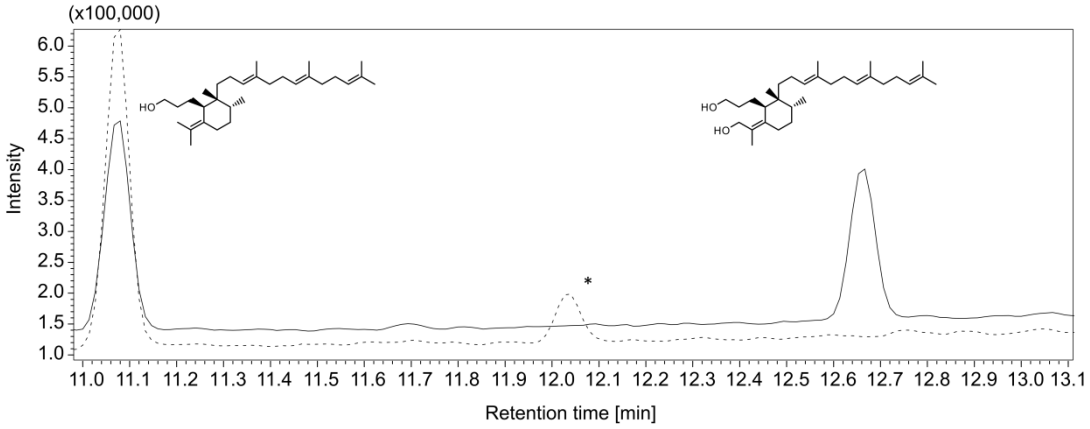

Figure 5

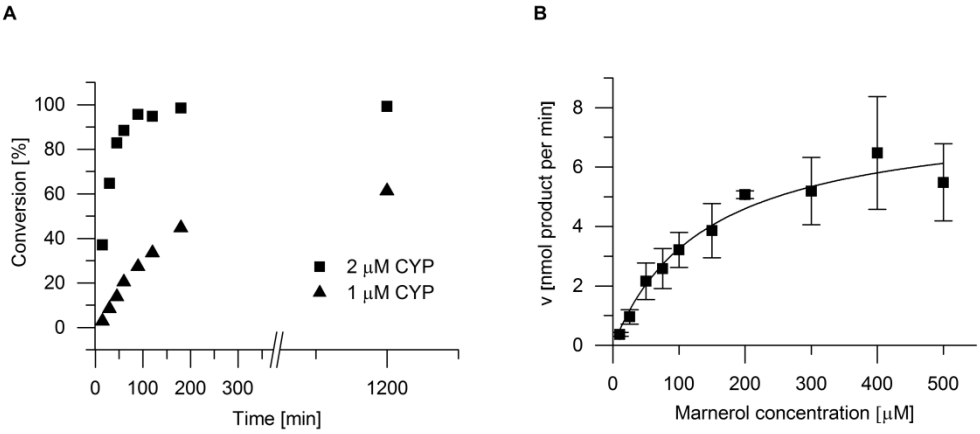

Figure 6

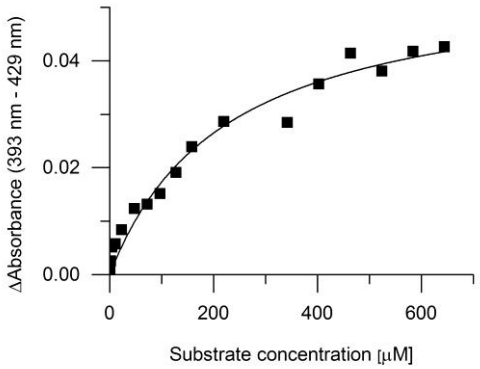

Figure 7

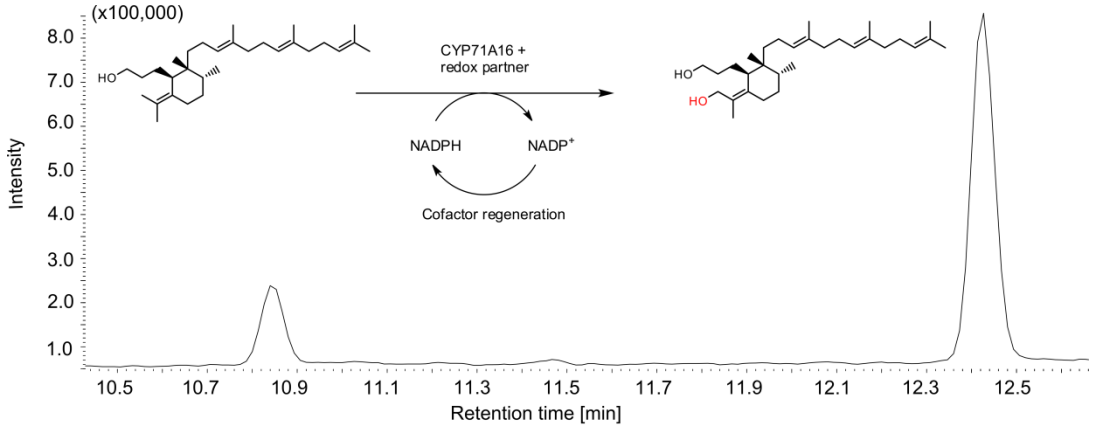

Graphical abstract

Highlights

- CYP71A16 from *A. thaliana* was expressed in modified form in *E. coli* at concentrations of up to 50 $mg \cdot L^{-1}$.
- CYP71A16 catalyzed the hydroxylation of the triterpenoid marnerol to form 23-hydroxymarnerol *in vitro*.
- K_M of 142.1 µM and a k_{cat} of 3.9 min^{-1} for marnerol oxidation by CYP71A16 were determined.
- CYP71A16 activity was supported by the reductase ATR2 from *A. thaliana* as well as by the bacterial redox partners Fpr and YkuN.